Journal of Electronic Materials
https://doi.org/10.1007/s11664-021-09221-y

ELECTRONIC PACKAGING AND INTERCONNECTIONS 2021

# Reliability of Ag Sinter-Joining Die Attach Under Harsh Thermal Cycling and Power Cycling Tests

**Zheng Zhang[1] · Chuantong Chen[1] · Aiji Suetake[1] · Ming-Chun Hsieh[1] · Katsuaki Suganuma[1]**

Received: 13 May 2021 / Accepted: 7 September 2021


**Abstract**
Silver (Ag) sinter-joining is an ideal connection technique for wide bandgap (WBG) power electronics packaging due to its excellent high-temperature stability and excellent thermal conductivity. In this work, we applied Ag sinter-joining to die attach for a WBG power module and focused reliability of Ag sinter-joining under harsh thermal and power cycling conditions. The die attach structure using a Ag flake paste had an initial shear strength of over 45 MPa due to the excellent sinter-joining ability of the paste. Variation of die attach shear strength and failure mode under a harsh cycling condition (−50~250 °C) have also been systematically discussed. Thermal diffusivity of sintered Ag and thermal resistance of the die attach structure were also measured, showing a superior thermal performance to solder materials. Meanwhile, a simple SiC diode module was assembled via Ag sinter-joining and aluminum (Al) ribbon-bonding for evaluation of Ag sinter-joining reliability during a severe power cycling condition. A power cycling test with a high junction temperature of 200 °C was conducted to evaluate the reliability of Ag sinter-joining. It is found that the main failure of the SiC diode module was located at ribbon-bonding rather than the Ag sinter-joining layer degradation, based on the variation of forward voltage and junction to case thermal resistance. This investigation indicates that the Ag sinter-joining has a long lifetime under a severe operating condition of power electronics.

**Keywords** Ag sinter-joining · thermal cycling · power cycling · reliability

## Introduction

Wide bandgap (WBG) semiconductors have a critical role in power electronics modules due to their excellent properties, such as high breakdown voltage, high junction temperature, and low on-resistance.[1–3] WBG power modules allow us to deal with an increasing power density and cut down power losses, which greatly benefit modern life and versatile usage of electricity. In the last decade, with the rapid development of WBG semiconductors, more and more apparatus, like electric motors, power transformers, and even tiny super-fast chargers, are equipped with WBG power modules. However, new challenges come along with the widespread applications of WBG power modules. A higher junction temperature of WBG semiconductors, even up to 250 °C, brings severe issues for the packaging of power electronics, especially for the packaging of die attach, which is the most critical part in power electronics.[4,5] Typically, the WBG semiconductor bonds to a substrate or lead frame via solder or a conductive adhesive. Although a decent bonding quality can be achieved by these traditional bonding materials, they are almost incapable of dealing with a severe junction temperature of over 250 °C. Currently, the Ag sinter-joining technique, which has excellent high-temperature resistance and electrical properties, is regarded as one of the promising approaches for the WBG die attach in power electronics.[6,7]

The Ag sinter-joining technique is based on sintering of Ag paste to realize bonding between the die and the substrate. The Ag paste, which is made from Ag particles and organic solvents, can be sintered into a continuous and uniform structure at a temperature below 250 °C. After sintering, it can also withstand severe high temperatures due to the high melting point of Ag. The sintered structure can also achieve a robust interconnection via an interdiffusion process at the bonding interface. Additionally, it has low electrical resistance on the order of $10^{-5}$ Ω cm and

✉ Zheng Zhang
zhangzheng@sanken.osaka-u.ac.jp

[1] Institute of Scientific and Industrial Research (SANKEN), Osaka University, Mihogaoka 8-1, Ibaraki, Osaka 567-0047, Japan

Published online: 11 October 2021

high thermal conductivity of over 200 W/m K on account of the superior electrical and thermal properties of Ag[8]. These merits perfectly meet the requirements for WBG die attach packaging, giving the Ag sinter-joining technology a significant advantage over traditional interconnection methods. In the last decade, massive efforts have been made on Ag sinter-joining for die attach packaging. For instance, Ag paste exhibits feasible bonding abilities on various surface metallizations, like Ag, Au, Ni, and Al, which significantly extend the application scenarios of Ag sinter-joining.[9–13] The bonding quality of die attach with Ag sinter-joining can reach a shear strength of over 40 MPa, showing a better initial bonding quality than soldering or adhesive joining.

Reliability is also critical for WBG power modules since the WBG semiconductors usually face high junction temperatures and severe temperature swings for a long time. The reliability of Ag solder-joining has been widely evaluated through different tests, such as thermal cycling, power cycling, and high-temperature storage.[14–16] Typically, the solder materials are susceptible to high temperatures that can lead to solder deterioration and alloy compound generation. Various reliability tests have also been conducted to investigate the performance of Ag sintering joining in harsh conditions. Yu et al. evaluated pressure-assisted Ag-sintered joints under severe test conditions (aging test: 300 °C; cycling test: −55~300 °C), [6] and their results suggest that the pressure-assisted joints have a shear strength of over 15.3 MPa after 2000 h thermal storage, and that the reliability of the sintered Ag layer is even superior to the reliability of a DBC substrate during the thermal cycling test. Zhang et al. added SiC particles into Ag paste, which significantly improved the reliability of the sintered Ag joints by restricting the grain growth of Ag during the thermal aging test.[17] Kim et al. conducted a quasi-power cycling test by using a SiC thermal engineering group chip with a temperature swing of 150 °C.[18] Based on the present research, Ag sinter-joining exhibits a decent reliability performance. However, the failure mechanism of Ag sinter-joining still needs to be further investigated and identified, especially the power cycling test, due to various failure modes in the power module.

In this work, we prepared sintered Ag joints via a Ag flake paste under a low-temperature and pressureless sintering condition. A thermal cycling test and a power cycling test were conducted to evaluate the reliability of the Ag sintered die attach joint. The sinter-joining ability of the Ag flake paste was studied initially to understand the sintering behavior and properties of the Ag flake paste. The thermal cycling test was conducted at a temperature range from −50 to 250 °C, and the power cycling test was carried out at an initial target junction temperature of 200 °C, with a high on–off junction temperature swing of 157 °C. After the cycling tests, the structure of the die attach was investigated via X-ray computed tomography (CT) using a microfocus 3-D CT X-Ray system (XVA-160N; Uni-Hite System) and scanning electron microscopy (SEM; SU-8020 Hitachi) inspection to identify weak points and structural changes. The thermal resistance of the SiC diode module was also measured by a T3ster (Mentor Graphics) to identify die attach layer changes during the power cycling test.

## Experiment

### Materials and Die Attach Packaging

The Ag paste, made from Ag flakes (Fukuda Metal Foil and Powder) and organic solvent (provided by Daicel), was applied as Ag sinter-joining material for connection between die and substrate. The die attach joint (Fig. 1a) was assembled by a dummy Si die (3 mm × 3 mm) and a direct bonding copper (DBC, 30 mm × 30 mm) for the evaluation of the bonding quality during the thermal cycling test. The surfaces of the Si and the DBC were sputtered with Ni (2 µm)/Ti (0.1 µm)/Ag (2 µm) layer by layer in order to be compatible with the Ag sinter-joining. A SiC power module was also prepared for a power cycling test. A specially designed DBC substrate (22 mm × 20 mm) and a SiC diode (4.7 mm

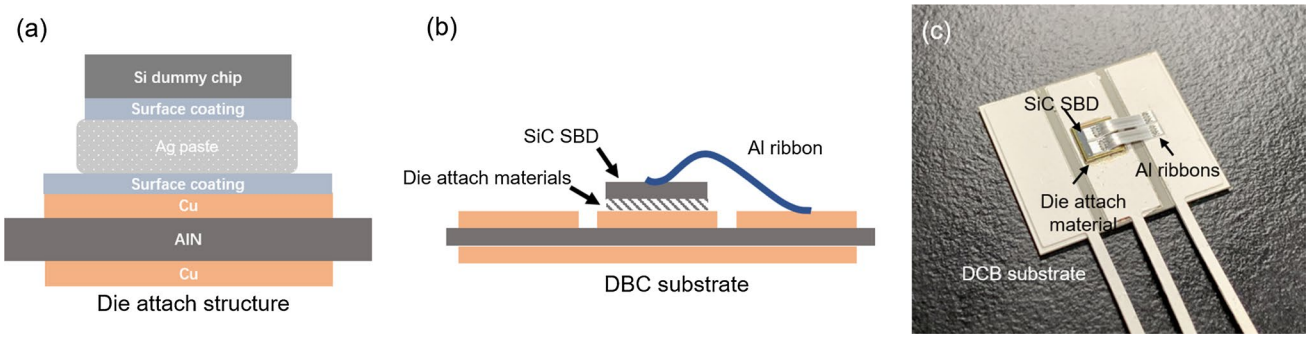


**Fig. 1** Schematics of the cross-section of die attach joint (a) and SiC diode module (b); image of the prepared SiC diode module (c)

× 4.7 mm) were applied for the assembly of a SiC diode module. For the Ag sinter-joining process, the Ag paste was printed on the substrate via a stencil-printed method with an initial printing thickness of 100 µm. The chips were then mounted on the printed Ag paste, and the specimens were heated on a hotplate at 250 °C for 60 min in the atmosphere. Topside bonding of the module was realized by Al ribbons (cross-section: 1.5 mm × 0.2 mm) through an ultrasonic bonding machine (TPT HB30). Schematics drawings of the SiC diode module cross-section and an image of the packaged module are shown in Fig. 1b and c, separately.

### Cycling Test Condition

The thermal cycling test and power cycling test were conducted to evaluate the reliability of the die attach joint with the Ag sinter-joining. The thermal cycling condition is schematically described in Fig. 2a, and was conducted in a temperature span from −50 to 250 °C. One cycle of the thermal cycling took 60 min with an equal dwell time (30 min) in a high-temperature and low-temperature chamber, respectively.

Power cycling was carried out via a power cycling tester (PST-2404; ESPEC), which contains a power supply, a stress current circuit, a measurement circuit, a switching system, and an air-cooling system. The schematic of the junction temperature and forward voltage variation during the cycling is shown in Fig. 2b. The cycling was conducted for a fixed time and in current mode. The junction temperature reached 200 °C after 3.25 s with a stress current of 47.6 A. Then, the SiC diode module was cooled to room temperature with a cooling time of 17 s via the air-cooling system.

### Characterizations

The thermal diffusivity of the sintered Ag flake paste was measured by a laser flash technique (LFA 467 Hyperflash; Netzsch). A sintered Ag pill-like cylinder structure was prepared in the same sintering conditions of the die attach for the measurement of its thermal diffusivity, and was measured from 25 °C to 175 °C. The shear strength of the sintered die attach was tested by a shear tester (Dage 4000) with a shear speed at 50 µm/s and a shear height at 100 µm. Four die attach joints were used to calculate the average shear strength. Cross-sections of the die attach before and after the thermal cycling test were initially polished via ion milling (IM-4000; Hitachi), and then observed by SEM and CT inspection of the die attach structure. The thermal resistance of the die attach was measured by a T3Ster with a heating current of 20 A and a measurement current of 0.05 A.

## Results and Discussion

### Sinterability of the Ag Paste

Typically, a decent sinterability plays an important role in sinter-joining, which is a pre-condition of a reliable connection as well as a good thermal performance. The sinterability of the Ag paste was firstly investigated via SEM by comparing the morphologies of the Ag particles and paste before and after sintering. Figure 3a presents the original morphologies of the Ag flakes, which show a flattened structure with irregular edges and shapes. After sintering, the flakes turn into a round-like structure with smooth edges, as shown in Fig. 3b. Meanwhile, some necks are generated among the scattered Ag flakes, which are able to provide connections in the sintered structure. Figure 3c exhibits a cross-section structure of the as-printed Ag paste. The Ag flakes are densely stacked layer by layer without any obvious gaps, due to the flattened structure of Ag. The sintered Ag cross-section structure is completely changed after the sintering, presenting a uniform porous structure, as shown in Fig. 3d. No Ag flakes are observed in the sintered structure, indicating complete sintering of the Ag paste. According to the SEM observations of the Ag paste, it can be confirmed that the Ag paste has an excellent sinterability under a pressureless and low-temperature sintering condition, which is arguably ascribed to the ball-milling process of the Ag flakes and the densely packaged Ag structure. The Ag flakes

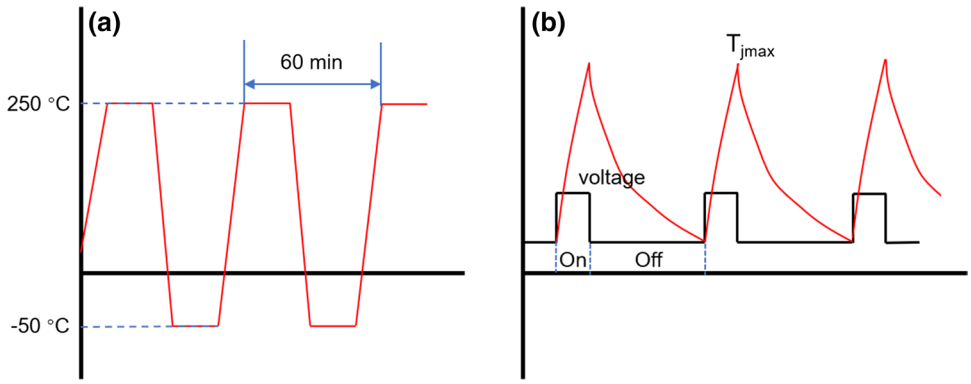


**Fig. 2** (a) Schematic of the thermal cycling profile with one cycling duration of 60 min; (b) schematic of the power cycling voltage variation (black curve) and the SiC diode junction temperature variation (red curve) (Color figure online)

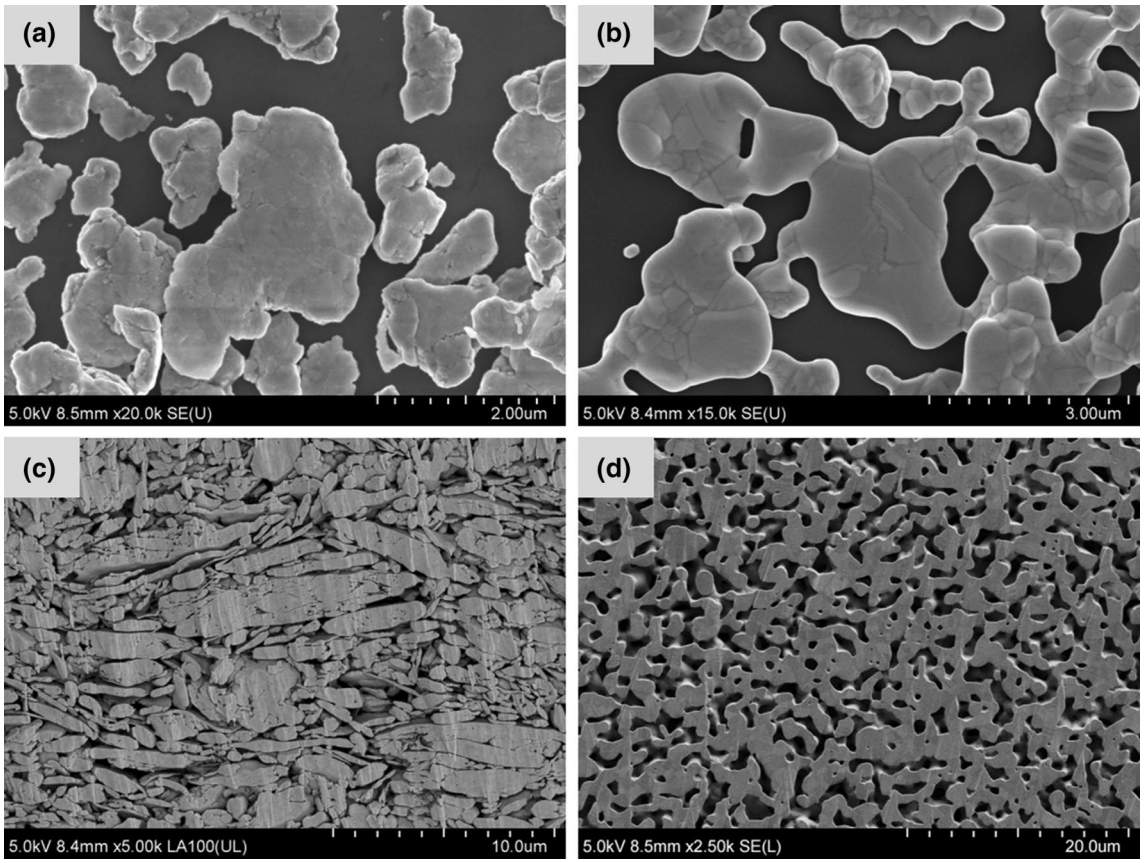


**Fig. 3** SEM images of Ag flakes and Ag paste cross-section: (a) original Ag flakes, (b) sintered Ag flakes, (c) cross-section of as-printed Ag paste, and (d) cross-section of sintered Ag paste

**Table 1** Average density and porosity of sintered Ag paste

| | Density | Porosity (%) |
|---|---|---|
| Sintered Ag paste | 6.20 g/cm$^3$ | 40.90 |
| Standard deviation | 0.101 g/cm$^3$ | 0.97 |

contain massive nano-subgrains and strains due to deformation generated during the ball-milling process.[19,20] During sintering, the nano-subgrains can significantly lower the melting temperature of the Ag flakes, and the strain energy in the flakes is able to facilitate the sintering process. Under the effects of the nano-subgrains and strain energy, the Ag flakes show a rapid and complete sintering process under a mild sintering condition. In addition, the densely printed flakes provide considerable connection areas compared to the conventional sphere particles, which is also beneficial for forming a dense sintered structure and necking procedure among the flakes.

The average density and porosity of the structure were measured on three different sintered Ag cylinder structures and are listed in Table 1. The density of the sintered Ag structure is calculated from the mass and size of the specimens. The porosity of the sintered Ag (∅) is calculated via Eq. (1) as follows:

$$\varnothing = 1 - \frac{\rho_{sintered}}{\rho_{solid}}, \tag{1}$$

where the $\rho_{solid}$ is the density of solid Ag (10.49 g/cm$^3$) and $\rho_{sinter}$ represents the density of the sintered Ag. The results indicate that the Ag paste possesses a dense sintered structure.

## Thermal Cycling Reliability of the Ag Sinter-Joining Die Attach

The shear strength variation of the die attach structure after the thermal cycling test is shown in Fig. 4. The shear strength of the as-sintered die attach can be over 45 MPa, which is notably superior to a die attach with solder or nano-Ag paste.[21–23] This is attributed to the excellent sinterability of the Ag flake paste, which is advantageous to the sintering bonding procedure between the die and the substrate. The shear strength of die attach gradually decreases to 30.1 MPa in the first 500 cycles. With a further increase of thermal

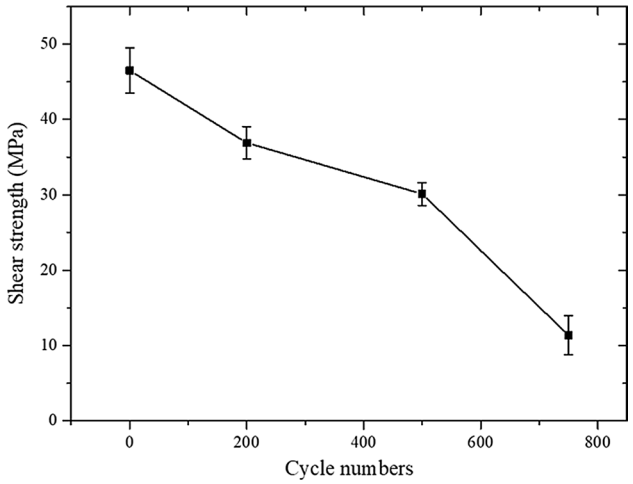


**Fig. 4** Variation of shear strength of die attach joints during the thermal cycling test

cycling numbers, a severe degradation in shear strength occurs and it reduces to 11.4 MPa after 750 cycles. The data of the shear test can be obtained in the supplementary Table S1. The harsh cycling condition can affect the microstructure of the die attach, causing thermal stress cracks or delamination in the structure.[18,24,25] Therefore, the cross-section and fracture surface of the die attach were investigated to understand its degradation.

Figure 5 shows topside X-ray CT images of the die attach before and after 750 thermal cycling cycles. Sintered Ag before cycling is evenly dispersed under the dummy die, while a small amount of Ag overflowed due to a mounting process (Fig. 5a). No obvious cracks can be recognized in the sintered Ag layer, which suggests an intact initial bonding structure. The die attach joint after 750 cycles shows a degraded Ag layer in which obvious cracks have been generated in the overflowed Ag structure, and the sintered Ag layer under the dummy die exhibits a crazing pattern, as shown in Fig. 5b. This is due to drastic thermal stress under a high stress condition that introduces microcracks when the porous Ag grows and coalesces.[26]

Cross-sections of die attaches before and after 750 cycles of thermal cycling are presented in Fig. 6. The cross-section of the as-sintered die attach joint appears as a homogenous Ag porous structure (Fig. 6a). With magnified observations of the top and bottom bonding interface (Fig. 6b and c), it can be seen that the sintered Ag has completely bonded to the surface metallization of the substrate and chip. The cross-section of the 750-cycled specimen exhibits a coarsened sintered structure with thick connection necks and larger pores, due to the diffusion of the Ag grains which occurs at high temperature and leads to growth and coarsening of the Ag.[26,27] As the sintered Ag layer is subjected to thermal cycling, the initial Ag structure gradually grows and coalesces to form large pores and interconnected microcracks, as seen in Fig. 6e. Meanwhile, the substrate shows a plastic deformation interface due to the drastic stress caused by the severe thermal shock. The two specimens show a different thickness in the sintered Ag layer, which is attributed to the manual printing and mounting process during specimen preparation. Figure 6f and g give magnified views of the top and bottom bonding interface, respectively. A delamination layer occurs at the interface between the dummy die and the sputtering layer, whereas the sintered Ag still intimately connects to the surface metallization at the bottom bonding.

Typically, the shear strength of a sintered Ag die attach gradually decreases during a thermal cycling test which is due to the large pores and interconnected microcracks after a severe cycling condition. However, there is a dramatic decrease in the shear strength of a die attach after 500 cycles, which is unusual according to reports.[28,29] This is arguably ascribed to the delamination located at the interface between the bare die and the sputtering layer. Due to the different Young's moduli of metal and Si, dramatic stress is concentrated at the interface between the dummy Si die and the sputtering layer during the harsh cycling conditions.[30] Under the influence of the mass stress, the interface between

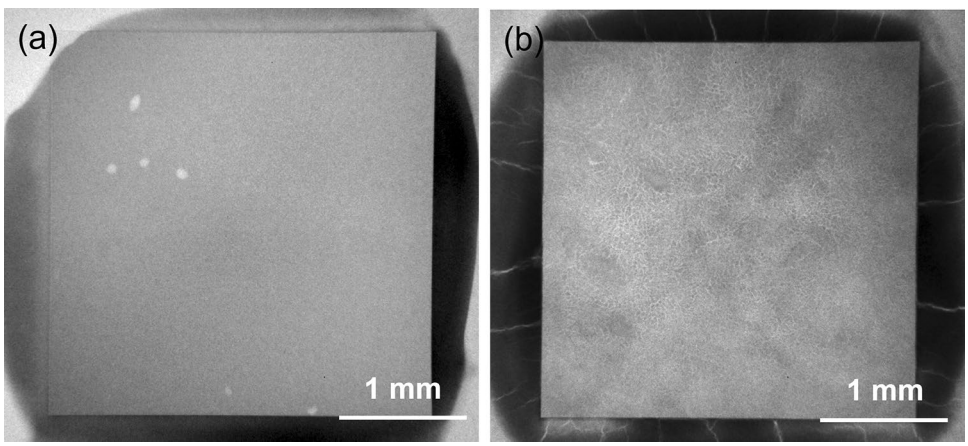


**Fig. 5** X-ray CT observations of die attach joint before (a) and after (b) 750 cycles of thermal cycling testing

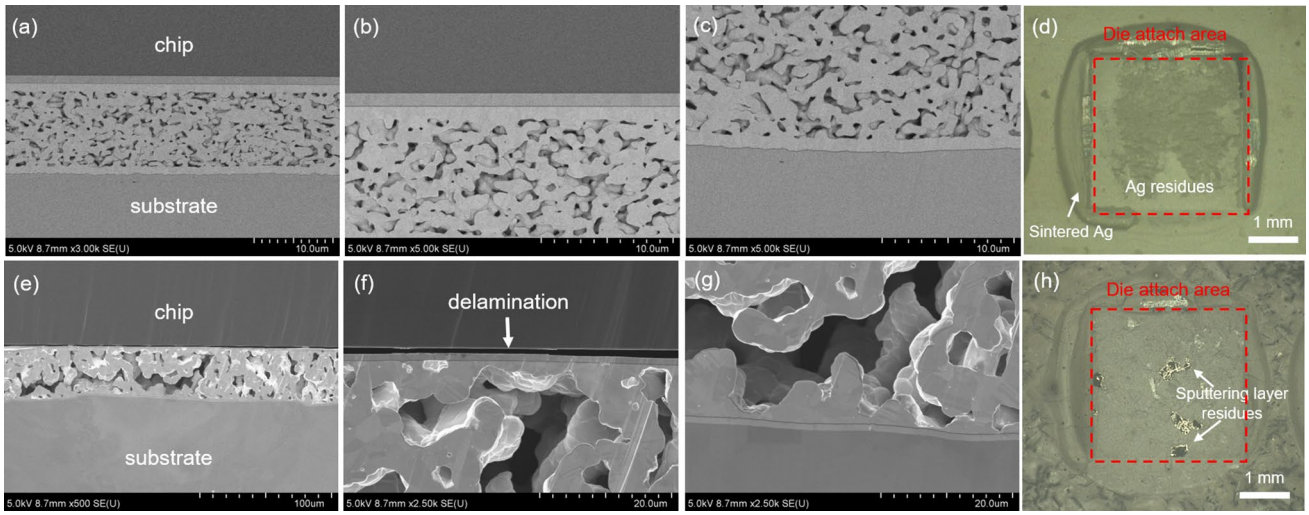


**Fig. 6** SEM cross-section and optical fracture surface images of the as-sintered die attach (a–d) and the 750-cycled die attach joint (e–h)

the dummy Si chip and the sputtering layer is a weak point, which is susceptible to delamination, and which significantly impairs the die attach joint, especially when the sputtering quality is not reliable or there is contamination on the surface of the die. In contrast, the bottom bonding interface is less influenced by the stress and thus still exhibits an intact structure on account of a similar Young's modulus of the Cu substrate and sintered Ag, as shown in Fig. 6g.

Fracture surfaces of sheared specimens are revealed in Fig. 6d and h. Massive Ag residues are observed on the substrate surface of the as-bonded specimen, which indicates that fractures in the sintered Ag layer are dominant. The fracture surface also confirms a decent bonding quality of the as-sintered die attach on account of the sturdy and flawless sintered Ag structure. Figure 6h presents the fracture surface of the 750-cycled specimen. There are some Ag and sputtering layer residues on the fracture surface, suggesting that fractures are not only located at the sintered Ag layer but also at the bonding interface between the bare chip and the sputtering layer. The fracture surface is in accordance with the observation of the joint cross-section where delamination and cracks have been generated in the die attach structure. Based on the CT and cross-section observations, it can be concluded that the degradation of the sintered die attach joints is attributed to a combined action of the sintered layer degradation and the sputtering layer delamination.

## Thermal Performance Comparison of Different Die Attach Materials

The thermal performance of the sintered Ag structure is the other critical index for evaluating the Ag paste. The thermal diffusivity of the sintered Ag structure is shown in Fig. 7. Sn96.5Ag3.0Cu0.5 (SAC305) solder and alumina

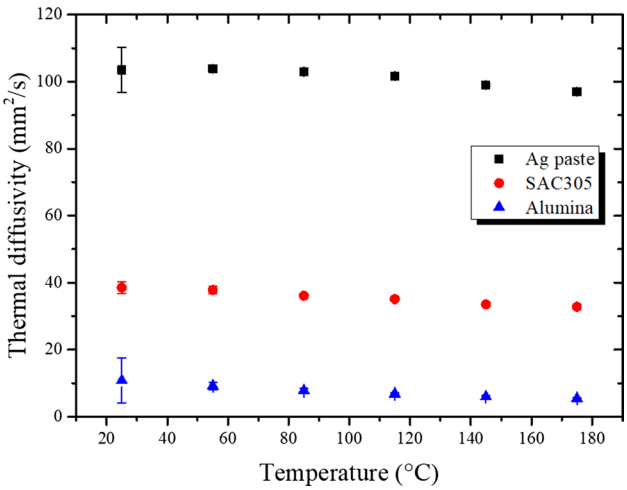


**Fig. 7** Thermal diffusivity of sintered Ag paste, SAC305, and alumina at different temperatures

were also measured for comparison. Even though the thermal diffusivity of the sintered Ag degrades compared to the solid Ag due to its porous structure, it remains at 105 $mm^2/s$ at room temperature (solid Ag 165.63 $mm^2/s$), which is over twice as much as the SAC305 solder (39 $mm^2/s$) and almost ten times that of alumina (11 $mm^2/s$). The high thermal diffusivity of the sintered Ag structure is mainly due to the continuous porous structure, as seen in Fig. 3b, which provides a thermal conduction pathway through the interconnected necks. The thermal diffusivity of different materials is reduced with an increase in temperature. However, the sintered Ag structure still possesses a high thermal diffusivity of around 100 $mm^2/s$, suggesting an excellent performance in thermal conduction even at high temperatures.

The thermal resistance of die attach with Ag paste joining was tested via a T3ster and compared with solder-sintered die attaches. Figure 8 depicts differential structure functions of the modules with Ag paste, AuSn solder, and SAC305 as the die attach material. The structure of the prepared module can be distinguished via the peak position of the curves. They present two obvious peaks with different gap distances, which correspond to the die attach layer in the joint. The thermal resistance of the sintered Ag paste layer is 0.050 K/W, which is much lower than that of AuSn (0.177 K/W) and SAC305 (0.123 K/W). The structure functions of the packaged module show that the Ag sinter-joining has a superior thermal performance to the solder materials.

## Power Cycling Reliability of Ag Sinter-Joining

The reliability of the Ag sinter-joining during harsh power cycling tests was also investigated, and the temperature variation of the case and junction are shown in supplementary Fig. S1. The junction temperature of the SiC diode module is calculated via the temperature coefficient of the diode, and the case temperature is directly measured through a thermal couple located at the bottom of the substrate. The power-on temperatures of the case and junction remain at around 40 °C, suggesting a complete cooling of the module. The temperature of the junction after power-on remains stable at the initial stage of the power cycling, and then gradually increases from 200 to 220 °C after 2901 cycles. Commonly, failures like lift-off of the bonding wire or degradation of the die attach layer can lead to an increase in the junction temperature. Therefore, we investigated the forward voltage ($V_f$) and the junction to case thermal resistance ($R_{th(j\text{-}c)}$) of the prepared module to identify the location of failures. The junction to case thermal resistance is calculated by Eq. (2) as follows:

$$R_{th(j-c)} = \frac{T_j - T_c}{P} \tag{2}$$

where $T_j$ and $T_c$ are the junction temperature and case temperature, respectively, after power off. $P$ represents the power consumption of the diode during power cycling[31].

As shown in Fig. 9, the $R_{th(j\text{-}c)}$ of the SiC diode module remains at around 0.7 K/W before 2600 cycles and shows an increase of around 0.037 K/W at the final stage of the power cycling. The thermal resistance of the module shows an increase of around 5.3% after 2901 cycles. Meanwhile, the $V_f$ of the diode gradually increases from the beginning of the power cycling and reaches 2.63 V at the end of cycling, exhibiting an increasing percentage of 13.4%. The significant increase of $V_f$ illustrates that degradation occurred even at the early stage of the power cycling test, which is regarded as evidence of ribbon bonding lift-off.[32]

Figure 10a and b shows the CT observations of the die attach layer before and after the power cycling test, respectively. There are a few voids in the sintered Ag layer seen in Fig. 10a, which are from air bubbles generated during the Ag paste printing process. The voids do not show any enlargement in volume and there are no obvious newly generated voids or microcracks in the die attach layer after the power cycling test, as shown in Fig. 10b. Unlike the thermal cycling test that has a large junction temperature swing of 300 °C, the junction temperature swing is about 160 °C (40~200°C), which is unable to cause severe degradation

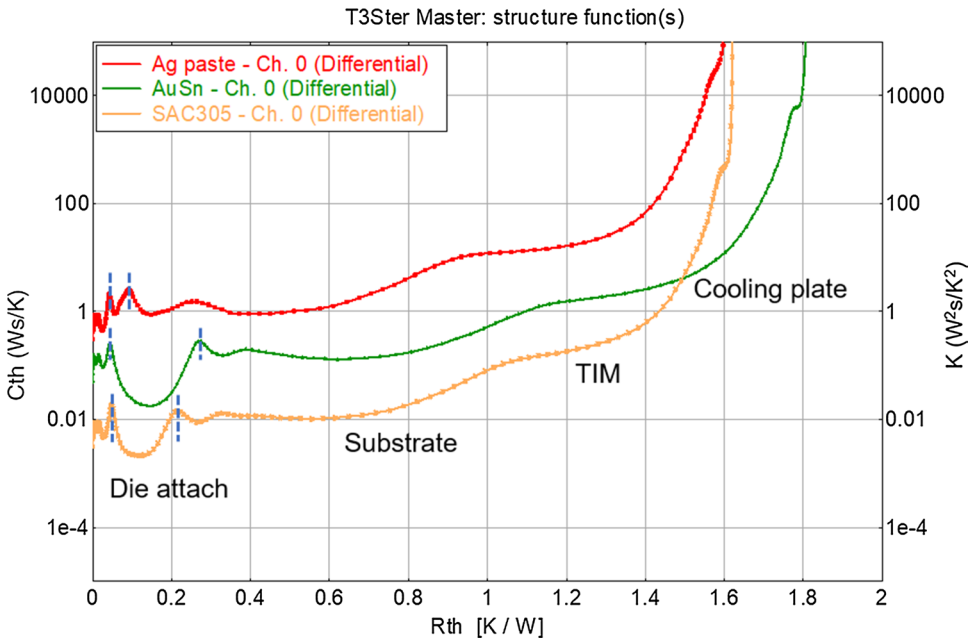


**Fig. 8** Differential structure functions of the prepared SiC diode module with different die attach materials

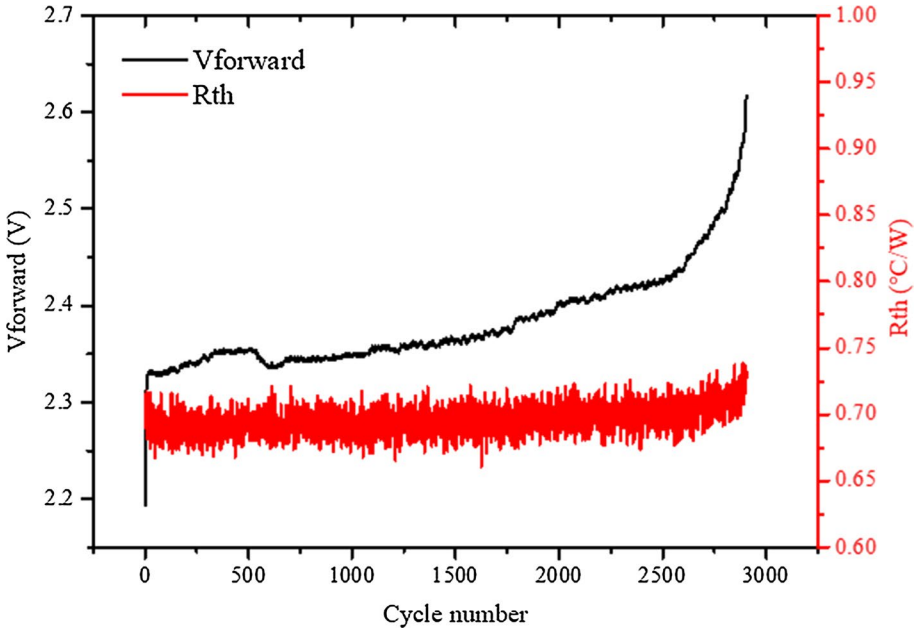


**Fig. 9** Forward voltage and junction to case thermal resistance variation during the power cycling test

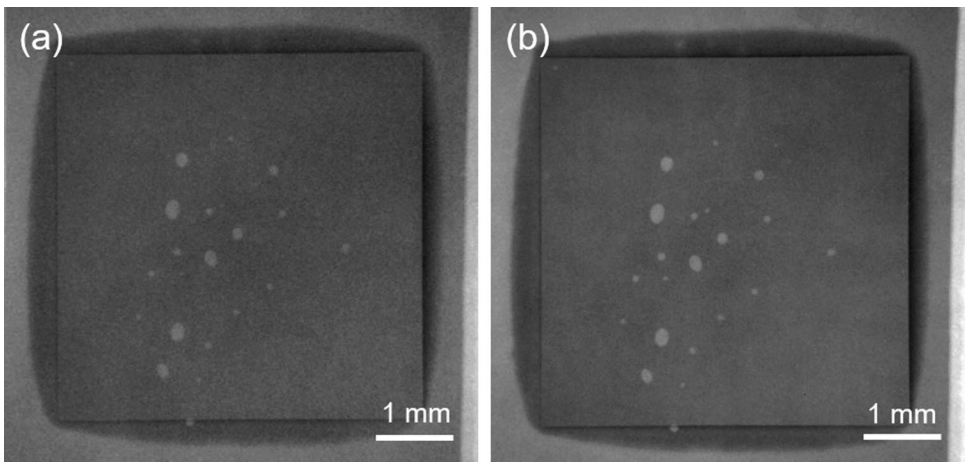


**Fig. 10** CT observations of the SiC diode module before (a) and after (b) power cycling test

in the sintered layer or sputtering layer delamination in the short power cycling test. According to the CT observation, it can be confirmed that there is excellent reliability of the Ag sinter-joining during the power cycling test, which is suitable for a high junction temperature of 200 °C.

Figure 11 shows structure functions of the SiC diode module before and after the power cycling. The structure functions show a similar tendency of variation regardless of the power cycling test. A slight increase in the thermal resistance of die attach structure is identified via the differential structure function, which is in accordance with the $R_{th(j\text{-}c)}$ increase in Fig. 9. For the wear-out failures of the power module, they are predominantly located in the ribbon-bonding and the die attach. [33,34] The different thermal expansion coefficients of the semiconductor materials and metals can generate severe thermal stress during cooling and heating, causing ribbon-bonding lift-off or die attach layer degradation. These two different failure modes play a combined action in the ultimate failure of the power module. On the one hand, the degradation in the die attach layer is able to lead to a higher junction temperature due to an increase in thermal resistance. The higher junction temperature introduces thermal stress at the ribbon-bonding interface, which accelerates ribbon-bonding lift-off on the topside. On the other hand, ribbon lift-off increases the forward voltage of the power module, and thus increases its power consumption. The increased power consumption results in a higher junction temperature, which can, in turn, lead to die attach layer deterioration such as microcracks and sputtering layer delamination.

In this experiment, the forward voltage increased prior to the thermal resistance and showed a larger increment

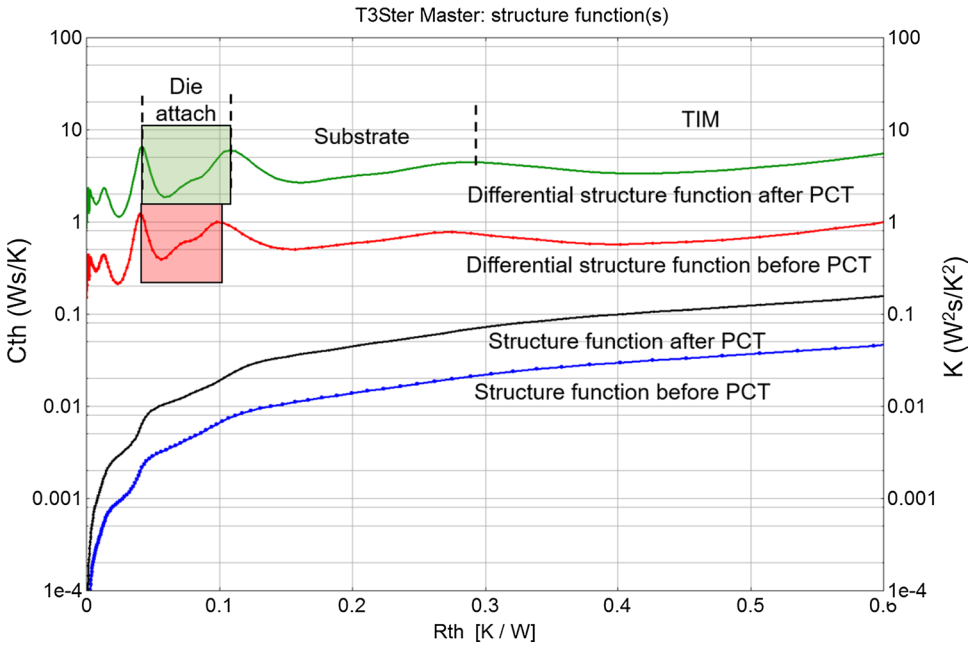


**Fig. 11** Structure functions of the Ag sinter-joining SiC diode module before and after the power cycling

than that of thermal resistance after power cycling due to the ribbon lift-off. With the further increase of the junction temperature, the die attach layer was slightly affected and showed a slight increase in the thermal resistance at the final stage of the power cycling. This result suggests that an initial failure occurred at the ribbon-bonding and played a major role in the malfunction of the SiC diode module.

## Conclusions

We have evaluated the thermal and power cycling reliability of Ag sinter-joining. The sinter-joining was achieved via a Ag flake paste, which has excellent sinter-joining ability and thermal diffusivity under a pressureless and low-temperature sinter-joining condition due to the ball-milling of the flake particles. The sintered die attach structure has a decent initial shear strength of over 45 MPa which reduces to 30.1 MPa in the first 500 cycles and drastically degrades to 11.4 MPa after 750 cycles under a cycling condition from −50 to 250 °C. It has been found that the degradation of the die attach structure is due to a combined action of degradation of the sintered Ag layer and delamination at the interface between the die and the sputtering layer. The thermal diffusivity and thermal resistance of the die attach structure with different connection materials were also measured and compared. The Ag sinter-joining revealed a better thermal performance than Sn-based solder materials. In addition, a power cycling test with an initial junction temperature of 200 °C was carried out to evaluate the reliability of the Ag sinter-joining. The junction temperature of the prepared SiC diode module gradually increased to 220 °C after 2901 cycles. The increase in junction temperature was mainly due to a ribbon lift-off at the initial stage of cycling, which was identified by the forward voltage and junction to case thermal resistance variation. Based on these results, it can be concluded that Ag sinter-joining has outstanding reliability compared to traditional die attach materials during thermal and power cycling test, and has a wide application scenario in high-temperature WBG power modules.

**Supplementary Information** The online version contains supplementary material available at https://doi.org/10.1007/s11664-021-09221-y.

**Acknowledgments** This paper is based on results obtained from a project (JPNP14004) commissioned by the New Energy and Industrial Technology Development Organization (NEDO). The author acknowledges the Network Joint Research Centre for Materials and Devices, Dynamic Alliance for Open Innovation Bridging Human, Environment and Materials.

## Declarations

**Conflict of interest** The authors declared that they have no conflict of interest.

## References

1. T.P. Chow, R. Tyagi, *Wide bandgap compound semiconductors for superior high-voltage power devices*, in: [1993] *Proceedings of the 5th International Symposium on Power Semiconductor Devices and ICs*, IEEE, (1993), p. 84
2. R. Wu, J. Wen, K. Yu, D. Zhao, *A discussion of SiC prospects in next electrical grid*, in: 2012 *Asia-Pacific Power and Energy Engineering Conference*, IEEE, (2012), p. 1

3. J. Millán, P. Godignon, X. Perpiñà, A. Pérez-Tomás, and J. Rebollo, *A survey of wide bandgap power semiconductor devices IEEE Trans. Power Electr.* 29, 2155 (2013).
4. H. Niu, *A review of power cycle driven fatigue, aging, and failure modes for semiconductor power modules*, in: 2017 *IEEE International Electric Machines and Drives Conference (IEMDC)*, IEEE, (2017), p. 1
5. V.R. Manikam, and K.Y. Cheong, *Die attach materials for high temperature applications: a review IEEE Trans. Compon. Packag. Manuf. Technol.* 1, 457 (2011).
6. F. Yu, R.W. Johnson, and M.C. Hamilton, *Pressureless sintering of microscale silver paste for 300°C applications IEEE Trans. Compon. Packag. Manuf. Technol.* 5, 1258 (2015).
7. E. Ide, S. Angata, A. Hirose, and K.F. Kobayashi, *Metal–metal bonding process using Ag metallo-organic nanoparticles Acta Mater.* 53, 2385 (2005).
8. K. Suganuma, S. Sakamoto, N. Kagami, D. Wakuda, K.-S. Kim, and M. Nogi, *Low-temperature low-pressure die attach with hybrid silver particle paste Microelectron. Reliab.* 52, 375 (2012).
9. T. Morita, Y. Yasuda, E. Ide, and A. Hirose, *Direct bonding to aluminum with silver-oxide microparticles Mater. Trans.* 50, 226 (2009).
10. T. Ogura, S. Takata, M. Takahashi, and A. Hirose, *Effects of reducing solvent on copper, nickel, and aluminum joining using silver nanoparticles derived from a silver oxide paste Mater. Trans.* 56, 1030 (2015).
11. Z. Zhang, C. Chen, Y. Yang, H. Zhang, D. Kim, T. Sugahara, S. Nagao, and K. Suganuma, *Low-temperature and pressureless sinter joining of Cu with micron/submicron Ag particle paste in air J. Alloys Compd.* 780, 435 (2019).
12. C. Chen, Z. Zhang, C. Choe, D. Kim, S. Noh, T. Sugahara, and K. Suganuma, *Improvement of the bond strength of Ag sinter-joining on Electroless Ni/Au plated substrate by a one-step preheating treatment J. Electron. Mater.* 48, 1106 (2019).
13. S. Soichi, and K. Suganuma, *Low-temperature and low-pressure die bonding using thin Ag-flake and Ag-particle pastes for power devices IEEE Trans. Compon. Packag. Manuf. Technol.* 3, 923 (2013).
14. K. Suganuma, S.-J. Kim, and K.-S. Kim, *High-temperature lead-free solders: Properties and possibilities JOM* 61, 64 (2009).
15. H. Ji, M. Li, S. Ma, and M. Li, *Ni3Sn4-composed die bonded interface rapidly formed by ultrasonic-assisted soldering of Sn/Ni solder paste for high-temperature power device packaging Mater. Design* 108, 590 (2016).
16. Y. Yamada, Y. Takaku, Y. Yagi, Y. Nishibe, I. Ohnuma, Y. Sutou, R. Kainuma, and K. Ishida, *Pb-free high temperature solders for power device packaging Microelectron. Reliab.* 46, 1932 (2006).
17. H. Zhang, S. Nagao, and K. Suganuma, *Addition of SiC particles to Ag die-attach paste to improve high-temperature stability; grain growth kinetics of sintered porous Ag J. Electron. Mater.* 44, 3896 (2015).
18. D. Kim, S. Nagao, C. Chen, N. Wakasugi, Y. Yamamoto, A. Suetake, T. Takemasa, T. Sugahara, and K. Suganuma, *On-line thermal resistance and reliability characteristic monitoring of power modules with Ag sinter joining and Pb, Pb-free solders during power cycling test by SiC TEG chip IEEE Trans. Power Electron.* 36, 4977 (2020).
19. D. Zhang, *Processing of advanced materials using high-energy mechanical milling Prog. Mater Sci.* 49, 537 (2004).
20. G. Khayati, and K. Janghorban, *The nanostructure evolution of Ag powder synthesized by high energy ball milling Adv. Powder Technol.* 23, 393 (2012).
21. X. Wang, Y. Mei, X. Li, M. Wang, Z. Cui, and G.-Q. Lu, *Pressureless sintering of nanosilver paste as die attachment on substrates with ENIG finish for semiconductor applications J. Alloys Compd.* 777, 578 (2019).
22. J. Li, C.M. Johnson, C. Buttay, W. Sabbah, and S. Azzopardi, *Bonding strength of multiple SiC die attachment prepared by sintering of Ag nanoparticles J. Mater. Process. Technol.* 215, 299 (2015).
23. A. Haque, B. Lim, A. Haseeb, H.H. Masjuki, *Die attach properties of Zn–Al–Mg–Ga based high-temperature lead-free solder on Cu lead-frame. J. Mater. Sci.: Mater. Electron.* 23, 115 (2012).
24. S. Sakamoto, T. Sugahara, K. Suganuma, *Microstructural stability of Ag sinter joining in thermal cycling. J. Mater. Sci.: Mater. Electron.* 24, 1332 (2012).
25. K. Siow, and S. Chua, *Thermal Cycling of Sintered Silver (Ag) Joint as Die-Attach Material JOM* 71, 3066 (2019).
26. I.L. Regalado, J.J. Williams, S. Joshi, E.M. Dede, Y. Liu, and N. Chawla, *X-ray microtomography of thermal cycling damage in sintered nano-silver solder joints Adv. Eng. Mater.* 21, 1801029 (2019).
27. R.M. German, *Coarsening in sintering: grain shape distribution, grain size distribution, and grain growth kinetics in solid-pore systems Crit. Rev. Solid State Mater. Sci.* 35, 263 (2010).
28. H. Zhang, S. Nagao, K. Suganuma, H.-j. Albrecht, K. Wilke, *Thermostable Ag die-attach structure for high-temperature power devices. J. Mater. Sci.: Mater. Electron.* 27, 1337 (2016).
29. D. Kim, C. Chen, S. Noh, S.-J. Lee, Z. Zhang, Y. Kimoto, T. Sugahara, K. Suganuma, *Development of high-strength and superior thermal shock-resistant GaN/DBA die attach structure with Ag sinter joining by thick Ni metallization. Microelectron. Reliab.* 100, 113380 (2019).
30. C. Chen, C. Choe, Z. Zhang, D. Kim, K. Suganuma, *Low-stress design of bonding structure and its thermal shock performance (− 50 to 250 °C) in SiC/DBC power die-attached modules. J. Mater. Sci.: Mater. Electron.* 29, 14335 (2018).
31. D. Schweitzer, H. Pape, L. Chen, *Transient measurement of the junction-to-case thermal resistance using structure functions: chances and limits,* in: 2008 *Twenty-fourth Annual IEEE Semiconductor Thermal Measurement and Management Symposium,* IEEE, 2008, p. 191.
32. B. Ji, V. Pickert, W. Cao, and B. Zahawi, *In situ diagnostics and prognostics of wire bonding faults in IGBT modules for electric vehicle drives IEEE Trans. Power Electron.* 28, 5568 (2013).
33. T. Hung, S. Chiang, C. Huang, C. Lee, and K. Chiang, *Thermal–mechanical behavior of the bonding wire for a power module subjected to the power cycling test Microelectron. Reliab.* 51, 1819 (2011).
34. V. Smet, F. Forest, J.-J. Huselstein, F. Richardeau, Z. Khatir, S. Lefebvre, and M. Berkani, *Ageing and failure modes of IGBT modules in high-temperature power cycling IEEE Trans. Ind. Electron.* 58, 4931 (2011).